

## Colloidal photonic superlattices

Rajesh Rengarajan,<sup>1</sup> Peng Jiang,<sup>2</sup> Diane C. Larrabee,<sup>1</sup> Vicki L. Colvin,<sup>2</sup> and Daniel M. Mittleman<sup>1,\*</sup>  
<sup>1</sup>*Electrical and Computer Engineering Department, Rice University, MS-366, 6100 Main Street, Houston, Texas 77005*  
<sup>2</sup>*Department of Chemistry, Rice University, MS-60, 6100 Main St., Houston, Texas 77005*

(Received 7 August 2001; published 30 October 2001)

We report on the fabrication and optical characterization of photonic superlattices comprised of sequentially grown stacks of colloidal photonic crystals. The superlattice periodicity induces the formation of minibands due to folding of the photonic band structure. This represents the first instance in which midgap states have been incorporated into a colloidal photonic crystal via a specifically engineered structural modification.

DOI: 10.1103/PhysRevB.64.205103

PACS number(s): 42.70.Qs, 78.66.-w, 81.16.Dn

The development of three-dimensional photonic crystals with stop bands in the visible and near-IR regions has attracted much attention recently, in part because of their potential value in the fabrication of photonic integrated circuits.<sup>1</sup> Photonic crystals with three-dimensional periodicity have been fabricated using a variety of lithographic and selective etching techniques,<sup>2-5</sup> holographic methods,<sup>5</sup> and colloidal self-assembly.<sup>6,7</sup> Unlike most other techniques, this latter method relies on either entropic or chemical forces to drive the self-assembly of micron-sized particles. The resulting crystals have a number of appealing features. They are readily fabricated in a large-area planar thin-film format with controllable thickness up to hundreds of repeating layers. In addition, self-assembly and templating techniques offer an impressive versatility with respect to the materials used in fabricating the crystals<sup>8-13</sup> as well as their structural morphology.<sup>14,15</sup>

One issue which has not yet been addressed in the fabrication of colloidal photonic crystals is that of engineered defects. There has been much work on the incorporation of specific types of structural defects into both two-dimensional and three-dimensional crystals. When photonic crystals are formed via lithographic or micromachining methods, both point and extended defects can naturally be built into the structure during the fabrication process. Such defects give rise to propagating modes lying within the forbidden gap in the photonic density of states. These modes are a crucial element in the development of photonic crystals as waveguides, resonant cavities for low-threshold lasers, or as other photonic devices.<sup>1,16-18</sup> However, in the case of self-assembled crystals, the fabrication of specific types of defects in specific locations within the periodic dielectric lattice is not so straightforward. As a result, the formation of mid-gap propagating modes in colloidal crystals is problematic.

Another approach to the controlled formation of states within the forbidden gap is to use an extended periodicity, in the form of an optical superlattice. The general properties of such systems were first described theoretically by Russell<sup>19,20</sup> and subsequently discussed by several authors.<sup>21-28</sup> Examples have been experimentally realized in one-dimensional structures, in both semiconductor multilayers<sup>21,29</sup> and in optical fiber gratings.<sup>30</sup> As in electronic superlattice structures, the properties of such systems are dictated by the interplay between the two superimposed periodicities, one corresponding to that of the underlying lat-

tice (with lattice parameter  $a$ ) and the second arising from an engineered multilayer structure, typically with a much longer length scale  $\Lambda$ . This longer periodicity introduces folding in the Brillouin zone and induces the formation of a series of minibands and corresponding midgap states.<sup>31</sup>

Here we report the observation of miniband formation in a colloidal crystal superlattice. To our knowledge, this is the first instance in which midgap states have been intentionally located in a colloidal crystal system. This result is promising not only for the eventual application of colloidal photonic crystals as optical elements, but also because these samples represent a new regime for optical superlattices. Most of the previous experimental studies of superlattice states have been based on one-dimensional fiber Bragg gratings.<sup>32</sup> In this case, the maximum modulation of the refractive index that can be achieved is quite small, on the order of  $10^{-3}$ . As a result, many periods of the photonic crystal are required in order to obtain a significant optical stop band. For this reason and also for practical reasons involving the methods used to form these structures, the length scale  $\Lambda$ , associated with the longer periodicity, is almost always much larger than that of the lattice parameter  $a$ .<sup>23</sup> Typical values for the ratio  $\Lambda/a$  are  $\sim 10^3$  in fiber gratings and  $\sim 10^2$  in the semiconductor multilayers. In contrast, superlattices formed using colloidal techniques can exhibit a much larger index contrast and, therefore, a much smaller separation of length scales.

The samples used in this study are based on the technique of convective self-assembly, in which a crystal of submicron silica spheres grows on a vertical substrate from a liquid suspension.<sup>6</sup> The superlattice structure is formed by the sequential deposition of colloidal photonic crystals using two alternating sizes of silica colloids.<sup>33</sup> Structures fabricated in this fashion offer all of the advantages of colloidal crystals, including simple and inexpensive fabrication from a wide range of materials, precise thickness control, planar thin-film formats, and long-range three-dimensional order with no grain boundaries.<sup>6</sup> Moreover, they provide a unique format for the study of photonic superlattices, because the dielectric contrast is on the order of 1. As a result, it is possible to obtain a large optical stop band and pronounced minibands even if  $\Lambda/a$  is on the order of 10 or less.

Figure 1 shows scanning electron microscope (SEM) images of cross-sectional views of a typical sample. These show macroporous polymer superlattices, formed by infiltrating the original silica superlattice structure with polysty-

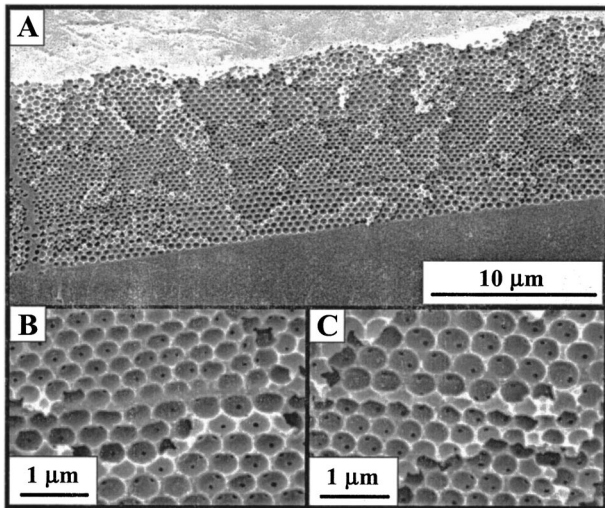


FIG. 1. SEM cross-sectional images of a typical colloidal superlattice. The silica colloidal crystal has been converted to a macroporous polymer, to facilitate imaging of the cross section. (a) A cross section of an ABA (three-layer) sample. (b) and (c) Close-up views of the AB and BA interfaces, respectively. These demonstrate that the interfaces are flat and uniform, even though the sphere diameters differ by more than 15%.

rene and then removing the silica spheres by etching to produce an inverted structure.<sup>11</sup> This process replicates the structure of the original silica films in a form amenable to cross-sectional imaging. These data clarify the morphology of the samples and permit us to accurately determine the radii of the spheres and the number of layers in each superlattice period. Also, they permit a careful evaluation of the quality of the interface between crystalline layers with different lattice constants. Figure 1(a) shows a cross-sectional view of an ABA structure, with three successive depositions. The two A sections consist of  $N_A = 11$  {111} lattice planes of a close-packed face-centered-cubic (fcc) colloidal crystal composed of 451-nm diameter spheres. The middle B section is  $N_B = 17$  {111} planes of an fcc crystal, with sphere diameter of 381 nm. The figure shows that both the A and B layers are planar and of uniform thickness throughout the structure and that the preferred vertical orientation of the {111} crystalline axis is preserved. Figures 1(b) and 1(c) show close-up views of the AB and BA interfaces, respectively. It is interesting to note that both interfaces are flat and well defined, indicating ordered growth of larger spheres on smaller ones and also of smaller spheres on larger ones. This somewhat surprising result holds for a fairly wide range of diameter ratios and permits us to fabricate a structure of arbitrary thickness by multiple depositions of alternating layers.<sup>33</sup> We have fabricated structures as thick as six layers (ABABAB).

The solid curves in Fig. 2 show the evolution of the normal-incidence transmission spectra as the number of repeat layers is increased. The lower two traces are single crystals of the A and B layers with numbers of lattice planes  $N_A = 11$  and  $N_B = 17$ , respectively. With only one layer (bottom spectra), the transmission shows a broad photonic stop band consistent with that observed for traditional colloidal crystals. When one size is layered on top of another, resulting

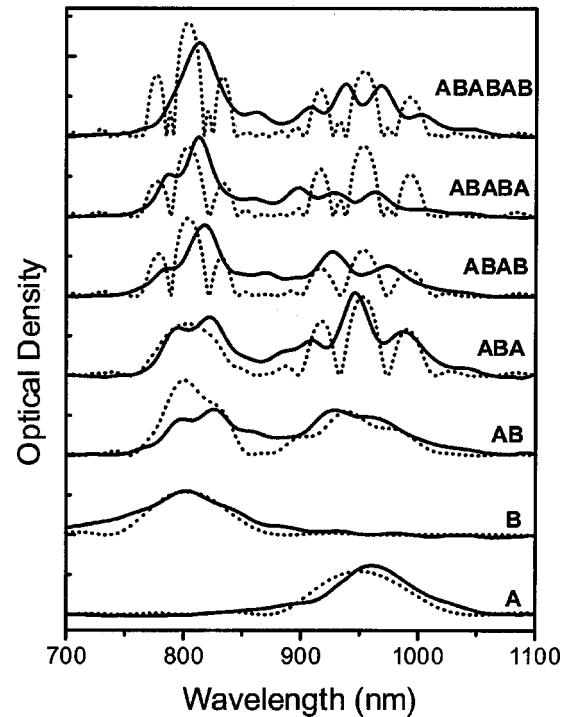


FIG. 2. The solid curves show normal-incidence optical density spectra of a series of films, in arbitrary units, vertically displaced for clarity. The lower two represent the spectra of an 11-layer film of the A spheres (451 nm) and a 17-layer film of the B spheres (381 nm), respectively. The remaining spectra are measured on samples with additional crystalline layers added alternately (AB, ABA, ABAB, etc.) as labeled. The dashed curves show the simulated spectra, calculated using the scalar-wave approximation. The parameters for each calculated curve are chosen to match those of the corresponding sample. With the exception of an overall multiplicative scaling for each curve, these simulations contain no adjustable parameters.

in an AB structure, two distinct stop bands with widths comparable to the individual layers are observed (third spectrum from the bottom). As the layering is repeated, however, each additional layer reinforces the long-range periodicity of the superlattice, resulting in significant modifications to the observed stop bands. In the thicker samples, the broad photonic stop bands exhibit pronounced modulation.

These general spectral features are similar to those observed in Moiré fiber Bragg gratings and are the hallmarks of an optical superlattice.<sup>24,26</sup> The superlattice periodicity in these films has the effect of modifying the original photonic band structure. This results in the folding of the band structure along the {111} direction in reciprocal space, leading to the formation of minibands. It should be noted that this zone folding description has generally been formulated with the assumption that the longer structural periodicity (of period  $\Lambda$ ) can be described as a slowly varying modulation of an unperturbed grating, with period  $a$ . In the structures described here, this description is not applicable, because the periodicity changes abruptly at each AB interface. Nonetheless, the general behavior is very similar to that observed in one-dimensional optical superlattices.

A simple description based on grating physics can provide

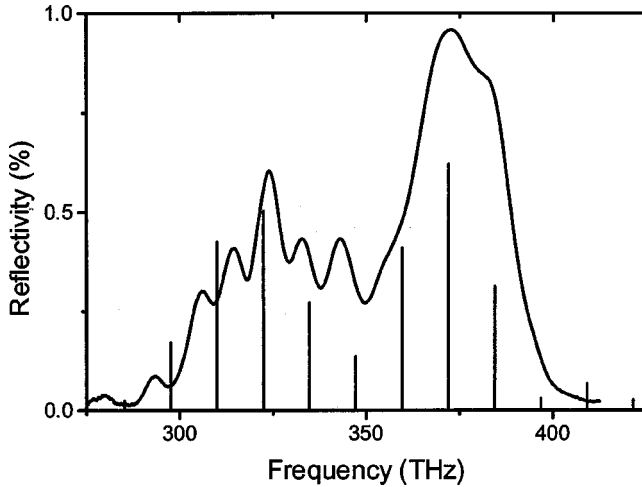


FIG. 3. The normal-incidence reflectivity of the ABABAB sample, derived from the optical density shown in Fig. 2. The stick spectrum represents the Fourier transform of the lowest-order approximation to the spatially varying dielectric function, as described in the text.

a qualitative understanding of the observed structure in the optical spectra of these films. The spectral positions of reflectivity peaks can be found from the lowest-order Fourier component of the spatially varying dielectric function  $\varepsilon(x)$ .<sup>21</sup> In our case, the amplitude of this component is constant (since the dielectric contrast in the *A* layers is the same as the dielectric contrast in the *B* layers), but the spatial period varies. So if the  $\{111\}$  lattice spacings for the *A* and *B* layers are denoted  $d_A$  and  $d_B$ , respectively, the lowest-order approximation to  $\varepsilon(x)$  can be written as  $\varepsilon_0 \cos(2\pi x/d_A)$  within the *A* layers and  $\varepsilon_0 \cos(2\pi x/d_B)$  within the *B* layers. The Fourier transform of this dielectric function contains a series of equally spaced sidebands, as a result of the frequency modulation. The sideband spectrum obtained in this fashion is shown in Fig. 3 along with the normal-incidence reflectivity of the thickest sample, derived from the optical density spectrum shown in Fig. 2. While the exact peak positions do not match precisely, we note that the general pattern and spacing of lines is in reasonable agreement. This peak spacing  $\Delta\nu$  is inversely related to the repeat distance of the superlattice,  $\Lambda = N_A d_A + N_B d_B$ , according to  $\Delta\nu = c/2n_0\Lambda$ , where  $n_0$  is the average refractive index of the crystal. This simple argument predicts a peak separation of  $\Delta\nu = 12.4$  THz, comparable to the experimentally determined value of  $9.2 \pm 1.0$  THz.

While this schematic description provides a useful starting point, it does not yield any information about the evolution of the optical spectrum with the thickness of the film. For this, more sophisticated calculations which describe the interaction of an electromagnetic field with a multiply periodic dielectric are required. As a first step towards this end,

we employ a scalar wave approximation,<sup>34</sup> in which scattering off of all except the  $\{111\}$  lattice planes is neglected. While this approximation is a severe one, it is worth noting that it has been shown to be reasonably accurate for modeling transmission line shapes as long as the propagation direction is along a high-symmetry direction of the lattice.<sup>35,36</sup> In order to model superlattice structures using the scalar-wave approach, we apply continuity boundary conditions to the scalar field and its derivative at each interface between crystals of different spheres and at the front and rear facets of the multilayer stack. The resulting system of linear equations can be solved by matrix inversion. These calculations assume values of  $N_A, N_B$ , and sphere diameters determined from SEM images and, therefore, contain no adjustable parameters other than multiplicative scaling factors.

The optical density spectra calculated in this fashion are shown in Fig. 2 (dotted curves). For the thicker samples, neither the modulation depth nor the spectral positions of the stop bands agree well with the simulations. This could be because of the accumulated effects of disorder in the fcc lattices or, more likely, because of small variations in the thicknesses of the uppermost layers relative to the underlying layers. Despite these discrepancies, the qualitative features of the experimental spectra are reproduced in these simulations. In particular, the simulations reproduce the fact that the *B* peak (at  $\sim 800$  nm) is not strongly modulated until the fourth layer is added to the sample (*ABAB*), while the *A* peak (at  $\sim 950$  nm) exhibits pronounced modulation when the third layer is added (*ABA*). The qualitative correspondence between this simple theory and the experimental results provides convincing evidence that the observed structure does indeed arise from superlattice effects.

In conclusion, we report the fabrication of a three-dimensional optical superlattice structure from sequential depositions of silica colloidal crystals by convective self-assembly. These samples represent the first examples of colloidal crystals with engineered midgap states and are therefore an important step in the development of photonic devices based on colloidal crystals. In contrast with other optical superlattice structures, these samples exhibit much higher index contrast and a much smaller superperiod. In principle, it should be possible to measure an optical stop band even if the superlattice period is as small as a few times the crystal lattice constant. These samples are also three-dimensional photonic crystals, which could lead to a unique interplay between the superlattice diffraction and higher-order Bragg diffraction phenomena.<sup>37</sup> They therefore offer an intriguing set of possibilities for engineering the optical properties of colloidal thin films.

This work has been partially supported by the National Science Foundation (CHE-967020) and the R. A. Welch foundation (C-1342).

- \*FAX: (713) 348-5686. Electronic address: daniel@rice.edu
- <sup>1</sup>J. D. Joannopoulos, R. D. Meade, and J. N. Winn, *Photonic Crystals: Molding the Flow of Light* (Princeton University Press, Princeton, NJ, 1995).
- <sup>2</sup>S. Y. Lin *et al.*, *Science* **394**, 251 (1998).
- <sup>3</sup>L. Zavieh and T. S. Mayer, *Appl. Phys. Lett.* **75**, 2533 (1999).
- <sup>4</sup>S. Noda *et al.*, *Science* **289**, 604 (2000).
- <sup>5</sup>M. Campbell *et al.*, *Nature* (London) **404**, 53 (2000).
- <sup>6</sup>P. Jiang *et al.*, *Chem. Mater.* **11**, 2132 (1999).
- <sup>7</sup>H. Miguez *et al.*, *Adv. Mater.* **10**, 480 (1998).
- <sup>8</sup>A. A. Zakhidov *et al.*, *Science* **282**, (1998).
- <sup>9</sup>J. Wijnhoven and W. L. Vos, *Science* **281**, 802 (1998).
- <sup>10</sup>A. Imhof *et al.*, *Phys. Rev. Lett.* **83**, 2942 (1999).
- <sup>11</sup>P. Jiang *et al.*, *J. Am. Chem. Soc.* **121**, 11630 (1999).
- <sup>12</sup>K. M. Kulinowski *et al.*, *Adv. Mater.* **12**, 833 (2000).
- <sup>13</sup>A. Blanco *et al.*, *Nature* (London) **405**, 437 (2000).
- <sup>14</sup>R. Rengarajan *et al.*, *Appl. Phys. Lett.* **77**, 3517 (2000).
- <sup>15</sup>P. Jiang, J. F. Bertone, and V. L. Colvin, *Science* **291**, 453 (2001).
- <sup>16</sup>V. Karathanos, A. Modinos, and N. Stefanou, *J. Phys.: Condens. Matter* **6**, 6257 (1994).
- <sup>17</sup>A. Chutinan and S. Noda, *Appl. Phys. Lett.* **75**, 3739 (1999).
- <sup>18</sup>S. Y. Lin *et al.*, *Opt. Lett.* **25**, 1297 (2000).
- <sup>19</sup>P. S. J. Russell, *J. Appl. Phys.* **59**, 3344 (1986).
- <sup>20</sup>P. S. J. Russell, *Phys. Rev. Lett.* **56**, 596 (1986).
- <sup>21</sup>V. Jayaraman, D. Cohen, and L. Coldren, *Appl. Phys. Lett.* **60**, 2321 (1992).
- <sup>22</sup>J. E. Sipe, L. Poladian, and C. M. de Sterke, *J. Opt. Soc. Am. A* **11**, 1307 (1994).
- <sup>23</sup>N. G. R. Broderick, C. M. de Sterke, and B. J. Eggleton, *Phys. Rev. E* **52**, 5788 (1995).
- <sup>24</sup>C. M. de Sterke and N. G. R. Broderick, *Opt. Lett.* **20**, 2039 (1995).
- <sup>25</sup>C. M. de Sterke, D. G. Salinas, and J. E. Sipe, *Phys. Rev. E* **54**, 1969 (1996).
- <sup>26</sup>N. G. R. Broderick and C. M. de Sterke, *Phys. Rev. E* **55**, 3634 (1997).
- <sup>27</sup>J. Zi, J. Wan, and C. Zhang, *Appl. Phys. Lett.* **73**, 2084 (1998).
- <sup>28</sup>F. Qiao, C. Zhang, and J. Wan, *Appl. Phys. Lett.* **77**, 3698 (2000).
- <sup>29</sup>H. Ishii *et al.*, *IEEE J. Quantum Electron.* **32**, 433 (1996).
- <sup>30</sup>C. M. de Sterke *et al.*, *Phys. Rev. E* **57**, 2365 (1998).
- <sup>31</sup>C. Weisbuch and B. Vinter, *Quantum Semiconductor Structures* (Academic, San Diego, 1991).
- <sup>32</sup>B. J. Eggleton *et al.*, *Electron. Lett.* **30**, 1620 (1994).
- <sup>33</sup>P. Jiang *et al.*, *Adv. Mater.* **13**, 389 (2001).
- <sup>34</sup>S. Satpathy, Z. Zhang, and M. R. Salehpour, *Phys. Rev. Lett.* **64**, 1239 (1990).
- <sup>35</sup>J. F. Bertone *et al.*, *Phys. Rev. Lett.* **83**, 300 (1999).
- <sup>36</sup>D. M. Mittleman *et al.*, *J. Chem. Phys.* **111**, 345 (1999).
- <sup>37</sup>H. M. van Driel and W. L. Vos, *Phys. Rev. B* **62**, 9872 (2000).